Synthesis and Anticancer Activity of Novel Benzimidazole and Benzothiazole Derivatives against HepG2 Liver Cancer Cells

Amal M. Youssef [1], Ahmed Malki[2], Mona H. Badr[1], Rasha Y. Elbayaa[1,*] and Ahmed S. Sultan [2,3,*]

[1]*Department of Pharmaceutical Chemistry, Faculty of Pharmacy, Alexandria University, Alexandria, Egypt*

[2]*Department of Biochemistry, Faculty of Science, Alexandria University, Alexandria, Egypt*

[3]*Department of Oncology, Georgetown University Medical Center, Washington DC, USA*

Abstract: Most of cancer chemotherapeutics and chemopreventives exert their effects by triggering apoptotic cell death. In this study, novel benzimidazole and benzothiazole derivatives have been synthesized to investigate their effects on HepG2 liver cancer cell lines after initial screening study. A dose response curve was constructed and the most active derivatives were further studied for apoptotic analysis. Six active benzimidazole derivatives (**8, 9, 10, 12, 13** and **14**) significantly induced apoptosis compared to control group. Two compounds **10** and **12** induced apoptosis by arresting cells in G1 phase of cell cycle which is confirmed by increased expression level of p21. The activity of caspase-3 which is well known as one of the key executioners of apoptosis was determined in the presence and absence of the tested derivatives. Our results indicated that compounds **10** and **12** significantly increased caspase-3 activity compared to control group. Moreover, a docked pose of compounds **10** and **12** was obtained bound to caspase-3 active site using Molecular Operating Environment module. This study demonstrated that benzimidazole derivatives **10** and **12** provoke cytotoxicity and induced apoptosis in liver cancer cells HepG2.

Keywords: Benzimidazole and benzothiazole derivatives/p21/Apoptosis/Caspase-3 activity/liver cancer.

INTRODUCTION

Cancer is a disease of striking significance in the world today. It represents the second leading cause of death, after cardiovascular diseases [1]. Hepatocellular carcinoma, a form of cancer originating in liver cells, is a challenging malignancy with high patient mortality rates worldwide [2]. Although therapies are available, drawbacks such as cytotoxicity have prompted researchers to seek more effective means of treatment. Chemotherapeutics are cytotoxic agents used to treat cancer. Ideally, these are developed to selectively cause toxicity to cancer cells with minimal cytotoxic effects to normal cells [3]. Given the toxicity, development of resistance, and lack of broad spectrum treatments, there is a continuing need for the development of new chemotherapeutic agents for the treatment of cancer. Accordingly, many diverse strategies have been employed to develop new therapies or to improve existing treatments. Literature survey revealed that, benzimidazole derivatives are endowed with different types of biological activities espically antitumor activity [4-7]. Pyrrolo[1,2-a]benzimidazoles represent a new class of antitumor agents exhibiting cytotoxic activity against a variety of cancer cell lines. The mechanism of cytotoxicity involves reductive alkylation of DNA accompanied by cleavage of G and A bases [8-15]. An anticancer agent, [Hoechst-33342], 2'-(4-ethoxyphenyl)-5-(4-methyl-1-piperazinyl)-2,5'-bis-1*H*-benzimidazole, has been demonstrated being an inhibitor of topoisomerase I [16,17]. Albendazole, a benzimidazole carbamate (methyl 5-propylthio-1*H*- benzimidazol-2-yl carbamate) with extensive clinical use as an anthelmintic drug, can also inhibit hepatocellular carcinoma cell proliferation under both in vitro and in vivo experimental conditions [18].

On the other hand, benzothiazole ring comprises a class of therapeutic compounds proved to exert a wide range of anticancer activity [19-23]. Literature survey revealed that, 2-(4-aminophenyl) benzothiazoles represent a new class of antitumor agents exhibiting inhibitory activity against human breast cancer cell lines [24-26].

Apoptosis is a selective process of physiological cell deletion that plays an important role in the balance between cellular replication and death. Apoptotic signaling can proceed via two pathways, i.e., via death receptors expressed on the plasma membranes of cells or alternatively via mitochondria, which contain several proteins that regulate apoptosis. The death receptor pathway is initiated by the ligation of membrane bound tumor necrosis factor (TNF) or Fas receptors, which result in a caspase-8-dependent cascade and subsequent cell death. During this cascade, caspase-8 cleaves BH3-interacting domain (Bid) and induces cytochrome c release and/or directly activates caspase-3 [27-29]. One of the key events in apoptosis is the activation of a cascade of intracellular cysteine proteases known as caspases. On proteolytic activation by upstream caspases, caspase-3 is able to cleave a variety of substrates, including poly (ADP-ribose)

*Address correspondence to these authors at the Department of Pharmaceutical Chemistry, Faculty of Pharmacy, Alexandria University, 1 Elkhartoum square-Azarita, 21521, Alexandria, Egypt; Tel: +2 (03) 4871317; Fax: +2 (03) 4873273; E-mail: rasha_bayaa@yahoo.com; Department of Biochemistry, Faculty of Science, Alexandria University, Alexandria, Egypt; E-mail: dr_asultan@univ.alex.edu.eg

1875-6638/12 $58.00+.00

polymerase (PARP). The cleavage of various substrates contributes to the typical morphological and biochemical features observed in apoptosis [30-32].

Encouraged by the above findings a number of benzimidazole and benzothiazole derivatives were synthesized and evaluated for their antitumor activity against liver cancer HepG2 cells. *In vivo* studies are in progress to investigate the mechanism of action of the interesting derivatives.

MATERIALS AND METHODS

Chemistry

Melting points were determined in open glass capillaries on a Gallenkamp melting point apparatus and were uncorrected. The infrared (IR) spectra were recorded on Perkin-Elmer 1430 infrared spectrophotometer using the KBr plate technique. ^{1}H-NMR spectra were determined on Jeol spectrometer (500 MHz) at the Microanalytical unit, Faculty of Science, Alexandria University using tetramethylsilane (TMS) as the internal standard and DMSO-d_6 as the solvent (Chemical shifts in δ, ppm). Splitting patterns were designated as follows: s: singlet; br s: broad singlet; d: doublet; t: triplet; q: quartet; m: multiplet. Microanalyses were performed at the Microanalytical Unit, Faculty of Science, Cairo University, Egypt and the found values were within ±0.4% of the theoretical values. Follow up of the reactions and checking the homogeneity of the compounds were made by TLC on silica gel-protected glass plates and the spots were detected by exposure to UV-lamp at 254 nm.

Ethyl 4-cyano-1-oxo-1*H*,5*H*-pyrido[2,1-b]benzimidazole-3-acetate (3) and ethyl 4-cyano-1-oxo-1*H*-pyrido[2,1-b]benzothiazole-3-acetate (4)

A mixture of 2-(1*H*-benzimidazol-2-yl)acetonitrile **1** or 2-(benzothiazol-2-yl)acetonitrile **2** (0.004 mole), diethyl acetone-1,3-dicarboxylate (0.81 g, 0.004 mole) and ammonium acetate (0,62 g, 0.008 mole) was heated in an oil bath at 140-150°C for 30-45 min; during this time ethanol and ammonia were liberated and the reaction mixture gradually solidified. After cooling, the solid was treated with ethanol and the product was filtered, washed with ethanol, dried and crystallized from the proper solvent.

Ethyl 4-cyano-1-oxo-1*H*,5*H*-pyrido[2,1-b]benzimidazole-3-acetate (3)

Yield: 67%, mp: 231-233 °C (Dioxane). IR (cm^{-1}): 3125 (NH); 2218 (C≡N); 1726, 1684 (C=O ester, C=O amide); 1529 (C=C). ^{1}H-NMR (δ ppm): 1.16 (t, *J* = 6.9 Hz, 3H, CH_2-C<u>H</u>$_3$); 3.11 (s, 2H, C<u>H</u>$_2$); 4.04 (q, *J* = 6.9 Hz, 2H, C<u>H</u>$_2$-CH_3); 6.36 (s, 1H, pyridobenzimidazole-C_2-<u>H</u>); 7.06-7.11 (m, 3H, pyridobenzimidazole-$C_{7,8,9}$-<u>H</u>); 7.21-7.22 (m, 1H, pyridobenzimidazole-C_6-<u>H</u>); 10.27 (s, 1H, NH, D_2O exchangeable). Anal. Calcd for $C_{16}H_{13}N_3O_3$ (295.29): C, 65.08; H, 4.44; N, 14.23. Found: C, 65.13; H, 4.65; N, 14.38.

Ethyl 4-cyano-1-oxo-1*H*-pyrido[2,1-b]benzothiazole-3-acetate (4)

Yield: 59%, mp: 182-184 °C (EtOH). IR (cm^{-1}): 2220 (C≡N); 1726, 1674 (C=O ester, C=O amide); 1510 (C=C); 1246, 1072 (C-S-C). ^{1}H-NMR (δ ppm): 1.23 (t, *J* = 6.95 Hz, 3H, CH_2-C<u>H</u>$_3$); 3.84 (s, 2H, C<u>H</u>$_2$); 4.25 (q, *J* = 6.95 Hz, 2H, C<u>H</u>$_2$-CH_3); 6.40 (s, 1H, pyridobenzothiazole-C_2-<u>H</u>); 7.50 (t, 1H, *J* = 7.65 Hz, pyridobenzothiazole-C_8-<u>H</u>); 7.57 (t, 1H, *J* = 7.65 Hz, pyridobenzothiazole-C_7-<u>H</u>); 7.85 (d, *J* = 8.4 Hz, 1H, pyridobenzothiazole-C_9-<u>H</u>); 8.28 (d, *J* = 7.65 Hz, 1H, pyridobenzothiazole-C_6-<u>H</u>). Anal. Calcd for $C_{16}H_{12}N_2O_3S$ (312.34): C, 61.53; H, 3.87; N, 8.97; S, 10.27. Found: C, 61.19; H, 3.65; N, 8.68. S, 10.34.

7,8,9,10-Tetrahydro-11-oxo-11*H*-benzothiazolo[3,2-b]isoquinoline-6-carbonitrile (5)

A mixture of 2-(benzothiazol-2-yl)acetonitrile **2** (0.70 g, 0.004 mole), ethyl cyclohexanone-2-carboxylate (0.68 g, 0.004 mole) and ammonium acetate (0,62 g, 0.008 mole) was heated in an oil bath at 140-150°C for 45 min; during this time ethanol and ammonia were liberated and the reaction mixture gradually solidified. After cooling, the solid was treated with ethanol and the product was filtered, washed with ethanol, dried and crystallized from dioxane. Yield: 76%, mp: 220-222 °C. IR (cm^{-1}): 2212 (C≡N); 1660 (C=O); 1543 (C=C); 1275, 1095 (C-S-C). ^{1}H-NMR (δ ppm): 1.68-1.70 (m, 4H, benzothiazoloisoquinoline-$C_{8,9}$-<u>H</u>$_2$); 2.62-2.64 (m, 4H, benzothiazoloisoquinoline-$C_{7,10}$-<u>H</u>$_2$); 7.52-7.55 (m, 2H, benzothiazoloisoquinoline-$C_{2,3}$-<u>H</u>); 8.04 (d, *J* = 7.65 Hz, 1H, benzothiazoloisoquinoline-C_1-<u>H</u>); 8.97 (d, *J* = 6.9 Hz, 1H, benzothiazoloisoquinoline-C_4-<u>H</u>). Anal. Calcd for $C_{16}H_{12}N_2OS$ (280.34): C, 68.55; H, 4.31; N, 9.99; S, 11.44. Found: C, 68.23; H, 4.65; N, 10.11; S, 11.62.

2-[4,6-Bis(4-chlorophenyl)-2-imino-1*H*-pyridin-3-yl]benzothiazole (6)

A mixture of 2-(benzothiazol-2-yl)acetonitrile **2** (0.35 g, 0.002 mole), 4-chlorobenzaldehyde (0.28 g, 0.002 mole), 4-chloroacetophenone (0.31 g, 0.002 mole) and ammonium acetate (1.23 g, 0.016 mole) in dry dioxane (5 ml) was heated under reflux for 12 hours. The solvent was evaporated under reduced pressure and the remaining solid was triturated with water, filtered, dried and crystallized from ethanol. Yield: 32%, mp: 118-120 °C. IR (cm^{-1}): 3421, 3282 (NH); 1610, 1527 (C=N, C=C); 1254, 1081 (C-S-C). ^{1}H-NMR (δ ppm): 7.49-7.51 (m, 3H, benzothiazole-$C_{4,5,6}$-<u>H</u>); 7.53 (s, 1H, pyridine-C_5-<u>H</u>); 7.64, 7.77 (2d, *J* = 8.4 Hz, each 2H, p-chlorophenyl-$C_{2,6}$-<u>H</u>); 7.91, 8.14 (2d, *J* = 8.4 Hz, each 2H, p-chlorophenyl-$C_{3,5}$-<u>H</u>); 8.24, 10.17 (2s, each 1H, N<u>H</u> and =N<u>H</u>, D_2O exchangeable); 8.27 (d, *J* = 7.65 Hz, 1H, benzothiazole-C_7-<u>H</u>). Anal. Calcd for $C_{24}H_{15}Cl_2N_3S$ (448.37): C, 64.29; H, 3.37; N, 9.37; S, 7.15. Found: C, 64.15; H, 3.63; N, 9.28; S, 6.96.

2-(1H-Benzimidazol-2-yl)acetimidohydrazide (7)

A mixture of compound **1** (7.2 g, 0.046 mole) and hydrazine hydrate (99%) (8.3 ml, 0.138 mole) was heated under reflux for 30 min. After cooling, the solid formed was triturated with ether, filtered, dried and crystallized from ethanol. Yield: 73%, mp: 231-233 °C. IR (cm^{-1}): 3482, 3316 (NH_2); 3142 (NH); 1626, 1541 (C=N, C=C). ^{1}H-NMR (δ ppm): 3.45 (br s, 2H, N<u>H</u>$_2$, D_2O exchangeable); 4.27 (s, 2H, C<u>H</u>$_2$); 5.10 (s, 1H, benzimidazole-N<u>H</u>, D_2O exchangeable), 6.35-6.37 (m, 2H, benzimidazole-$C_{5,6}$-<u>H</u>), 6.47-6.49 (m, 2H, benzimidazo-

le-$C_{4,7}$-H). Anal. Calcd for $C_9H_{11}N_5$ (189.22): C, 57.13; H, 5.86; N, 37.01. Found: C, 57.23; H, 5.74; N, 37.12.

General Procedure for the Preparation of Compounds 8, 9 and 10

A solution of compound **7** (1.5 g, 0.008 mole) in ethanol (30 ml) was treated with sodium ethoxide (1.84 g, 0.08 mole sodium metal in 10 ml ethanol). Thionyl chloride, ethyl chloroformate or ethyl bromoacetate (0.008 mole) was gradually added and the reaction mixture was stirred at room temperature for 1-2 hours during which a yellowish white crystalline product was separated. The product was filtered, washed with ethanol, dried and crystallized from methanol.

4-((1*H*-Benzimidazol-2-yl)methyl)-2,3-dihydro-1,2,3,5-thiatriazol-1-oxide (8)

Yield: 71%, mp: 267-269 °C. IR (cm^{-1}): 3413, 3165 (NH); 1619, 1539 (C=N, C=C); 1383 (SO). ^{1}H-NMR (δ ppm): 3.40 (s, 2H, C$\underline{H}_2$), 5.03 (s, 1H, benzimidazole-N$\underline{H}$, D_2O exchangeable), 6.30-6.31 (m, 2H, benzimidazole-$C_{5,6}$-H), 6.38-6.44 (m, 2H, benzimidazole-$C_{4,7}$-H). Anal. Calcd for $C_9H_9N_5OS$ (235.27): C, 45.95; H, 3.86; N, 29.77; S, 13.63. Found: C, 45.87; H, 3.82; N, 29.53; S, 13.42.

5-((1*H*-Benzimidazol-2-yl)methyl)-1*H*-1,2,4-triazol-3(2H)-one (9)

Yield: 56% , mp: > 300 °C. IR (cm^{-1}): 3440, 3180 (NH); 1681 (C=O); 1617, 1520 (C=N, C=C). ^{1}H-NMR (δ ppm): 3.42 (s, 2H, C$\underline{H}_2$), 5.13 (s, 1H, benzimidazole-N$\underline{H}$, D_2O exchangeable), 6.33-6.35 (m, 2H, benzimidazole-$C_{5,6}$-H), 6.48-6.50 (m, 2H, benzimidazole-$C_{4,7}$-H). Anal. Calcd for $C_{10}H_9N_5O$ (215.21) C, 55.81; H, 4.22; N, 32.54. Found: C, 55.72; H, 4.11; N, 32.66.

3-((1*H*-Benzimidazol-2-yl)methyl)-1,2-dihydro-1,2,4-triazin-5(6H)-one (10)

Yield: 69% , mp: > 300 °C. IR (cm^{-1}): 3428, 3180 (NH); 1685 (C=O); 1621, 1528 (C=N, C=C). ^{1}H-NMR (δ ppm): 3.63 (s, 2H, C$\underline{H}_2$), 4.52 (s, 2H, triazine-C_6-$\underline{H}_2$), 6.21 (s, 1H, benzimidazole-N$\underline{H}$), 6.59-6.61 (m, 2H, benzimidazole-$C_{5,6}$-H), 6.81-6.84 (m, 2H, benzimidazole-$C_{4,7}$-H), 12.00 (s, 1H, N$\underline{H}$, D_2O exchangeable). Anal. Calcd for $C_{11}H_{11}N_5O$ (229.24): C, 57.63; H, 4.84; N, 30.55. Found: C, 57.60; H, 4.74; N, 30.67.

N-(1*H*-Benzimidazol-2-yl)-1*H*-imidazole-1-carboxamide (12)

A solution of 1,1'-carbonyldiimidazole (1.33 g, 0.01 mole) and 2-amino-1*H*-benzimidazole **11** (1.62 g, 0.01 mole) in acetonitrile (50 ml) was stirred at room temperature for 20 h. The resulting precipitate was filtered, washed with ethanol, dried and crystallized from N,N-dimethylformamide (DMF). Yield: 68%, mp: > 300 °C. IR (cm^{-1}): 3335 (NH); 1630 (C=O); 1608, 1593 (C=N, C=C). ^{1}H-NMR (δ ppm): 6.94-6.97 (m, 2H, benzimidazole-$C_{5,6}$-H); 7.03-7.05 (m, 2H, benzimidazole-$C_{4,7}$-H); 7.37-7.51 (m, 2H, imidazole-$C_{4,5}$-H); 8.10 (s, 1H, imidazole-C_2-H); 11.71 (s, 1H, N$\underline{H}$, D_2O exchangeable). Anal. Calcd for $C_{11}H_9N_5O$ (227.22): C, 58.14; H, 3.99; N, 30.82. Found: C, 58.13; H, 3.65; N, 31.27.

General Procedure for the Preparation of Compounds 13, 14 and 15

A solution of **12** (0.45 g, 0.002 mole) and the appropriate amine (0.002 mole) in DMF (5 ml) was stirred at 100 °C for 2 h. The white solid obtained after cooling was filtered, washed with ethanol, dried and crystallized from the proper solvent.

1-(4-Methoxyphenethyl)-3-(1*H*-benzimidazol-2-yl)urea (13)

Yield: 71%, mp: 285-287 °C (DMF). IR (cm^{-1}): 3237, 3124 (NH); 1642 (C=O); 1608, 1553 (C=N, C=C); 1258, 1153, 1074 (C-O-C). ^{1}H-NMR (δ ppm): 2.70 (t, *J* = 6.9 Hz, 2H, C$\underline{H}_2$); 3.32 (t, *J* = 6.9 Hz, 2H, C$\underline{H}_2$); 3.68 (s, 1H, OC$\underline{H}_3$); 6.84 (d, *J* = 8.4 Hz, 2H, *p*-methoxyphenyl-$C_{3,5}$-H); 6.96-6.98 (m, 2H, benzimidazole-$C_{5,6}$-H); 7.14 (d, *J* = 8.4 Hz, 2H, *p*-methoxyphenyl-$C_{2,6}$-H); 7.28-7.30 (m, 2H, benzimidazole-$C_{4,7}$-H); 9.93, 11.49 (2s, each 1H, 2 N$\underline{H}$, D_2O exchangeable). Anal. Calcd for $C_{17}H_{18}N_4O_2$ (310.35): C, 65.79; H, 5.85; N, 18.05. Found: C, 66.13; H, 5.65; N, 18.38.

1-(1*H*-Benzimidazol-2-yl)-3-cyclohexylurea (14)

Yield: 65%, mp: > 300 °C (DMF). IR (cm^{-1}): 3329, 3146 (NH); 1640 (C=O); 1620, 1571 (C=N, C=C). ^{1}H-NMR (δ ppm): 1.18-1.31 (m, 4H, cyclohexyl-$C_{3,5}$-$\underline{H}_2$); 1.48-1.50 (m, 2H, cyclohexyl-C_4-$\underline{H}_2$); 1.62-1.80 (m, 4H, cyclohexyl-$C_{2,6}$-$\underline{H}_2$); 3.51-3.53 (m, 1H, cyclohexyl-C_1-H); 6.95-6.98 (m, 2H, benzimidazole-$C_{5,6}$-H); 7.30-7.32 (m, 2H, benzimidazole-$C_{4,7}$-H); 9.69, 11.42 (2s, each 1H, 2 N$\underline{H}$, D_2O exchangeable). Anal. Calcd for $C_{14}H_{18}N_4O$ (258.32): C, 65.09; H, 7.02; N, 21.69. Found: C, 65.13; H, 7.05; N, 21.45.

1-(1*H*-Benzimidazol-2-yl)-3-(4-methoxyphenyl)urea (15)

Yield: 54%, mp: > 300 °C (DMF/EtOH). IR (cm^{-1}): 3336, 3136 (NH); 1645 (C=O); 1611, 1573 (C=N, C=C); 1264, 1149, 1067 (C-O-C). ^{1}H-NMR (δ ppm): 3.72 (s, 1H, OC$\underline{H}_3$); 6.73 (d, *J* = 8.4 Hz, 2H, *p*-methoxyphenyl-$C_{3,5}$-H); 6.96-6.99 (m, 2H, benzimidazole-$C_{5,6}$-H); 7.39-7.35 (m, 2H, benzimidazole-$C_{4,7}$-H); 7.64 (d, *J* = 8.4 Hz, 2H, *p*-methoxyphenyl-$C_{2,6}$-H); 9.72, 11.69 (2s, each 1H, 2 N$\underline{H}$, D_2O exchangeable). Anal. Calcd for $C_{15}H_{14}N_4O_2$ (282.30): C, 63.82; H, 5.00; N, 19.85. Found: C, 64.10; H, 4.69; N, 19.68.

Anticancer Studies

Cell Culture and Drug Treatment

HepG2 cells were maintained in Dulbecco's modified essential media (DMEM, Gibco) supplemented with 10 % Fetal Bovine Serum (FBS), 100 Units/ml penicillin and 100 μg/ml streptomycin at 37°C in a 5% CO_2 atmosphere.

Cell Proliferation (MTT Assay)

4000- 5000 cells/well in 100 μL of medium were seeded in a 96-well plate for 24 h prior to drug treatment. The media was then changed to media with tested compounds. At the end of incubation (24 h), 10 μL of 5 mg/ml 3-(4,5-Dimethylthiazol-2-yl)-2,5-diphenyltetrazolium bromide (ATCC) was added to each well for 4 h. After incubation, 100 μL of 0.01 M HCl to one tube containing 1 gm of SDS was added to each well to dissolve the formazan crystals.

The absorbance was determined at 570 nm. Assays were performed in triplicate and standard deviation determined.

Enzyme Linked Immunosorbent Apoptosis Assay

Cells were seeded at a density of 2 X 10^4/ well in a 96-well plate and incubated for 24 hours. Media was changed to media containing the tested drugs (IC_{50} = 0.2~ 0.25 mM) dose. Cells then incubated for extra 24 hours. An ELISA assay was performed, using Cell Death Detection ELISA^{PLUS} kit (Roche-Applied Science, Indianapolis, USA) that measures histone release from fragmented DNA in apoptosing cells. Cells were treated with 200-µL lysis buffer for 30 min at room temperature. Cells lysate was subjected to centrifugation for 10 min and 200 µL of supernatant was collected, of which 20-µL was incubated with anti-histone biotin and anti-DNA peroxidase at room temperature for 2 h. After washing with incubation buffer three times, 100 µL of substrate solution (2, 2`azino-di (3-ethylbenzthiazolin-sulphuric acid) was added to each well and incubated for 15-20 min at room temperature. The absorbance was measured using an ELISA reader (Spectra Max Plus) at 405 nm. Each assay was done in triplicate and standard deviation was determined.

Caspase-3 Activity

Caspase-3 activity was assayed according to manufacturer's protocol (Assay designs, USA). 5X10^6 cells were lysed in 100 µL lysis buffer containing 10 mM HEPES (4-(2-hydroxyethyl)-1-piperazineethanesulfonic acid), pH 7.4, 2 mM EDTA, 0.1% CHAPS (3-[(3-cholamidopropyl)dimethylammonio]-1-propanesulfonicacid, 5 mM, 350 µg/ml PMSF (phenylmethanesulfonylfluoride or phenylmethylsulfonyl fluoride) and 5 mM DTT (Dithiothreitol). Cell were homogenized by three cycles of freezing and thawing and then centrifuged to remove the cellular debris. Each sample was then incubated in buffer containing 10 mM HEPES, pH 7.4, 2 mM EDTA, 0.1% CHAPS, 5 mM EDTA supplemented with its substrate (Ac-Asp-Glu-Val-Asp-AFC) Ac-DEVD-AFC for 1 hour at room temperature and then reaction was stopped with 1N HCl. OD_{405} was measured using a spectrophotometer (Spectra Max Plus). Each assay was done in triplicate and standard deviation was determined.

Flow Cytometric Analysis

Cells were seeded at a density of 3-5 X 10^5/ 10-cm^2 plate and incubated for 24 h before radiation. Media was changed to media containing **10** and **12** (200 µM), 30 min before irradiation. After 24 hours, cells were harvested by trypsinization. The cells were washed with PBS and fixed with ice-cold 70 % ethanol while vortexing. Finally, the cells were washed and resuspended in phosphate buffer saline (PBS) containing 5 µg/mL RNase A (Sigma, St. Louis, MO USA) and 50 µg/mL propidium iodide (Sigma, St. Louis, MO USA) for analysis. Cell cycle analysis was performed using FACScan Flow Cytometer (Becton Dickson) according to the manufacturer's protocol.

Western Blot Analysis

For p21 protein analysis, HepG2 cells were grown to 60% confluency and then the culture media was switched to media supplemented with 10 mM Metformin and/or 10 µM of MEK inhibitor I (Calbiochem; San Diego, CA) (26,27). After 24 h, cells were lysed with lysis buffer (10 mM Tris HCl pH 7.5, 1 mM EDTA, 1% triton X-100, 150 mM NaCl, 1 mM dithiothretol, 10% glycerol, 0.2 mM phenylmethysulphonyl fluoride and protease inhibitors). Protein concentrations were determined using BCA protein assay kit (Pierce; Rockford, IL). 20 µg of total protein was loaded to 8% sodium dodecyl sulphate – polycrylamide gel electrophoresis (SDS-PAGE) gels. The protein of interest was probed using anti-p21 (B-9) mouse IgG (Santa Cruz; Santa Cruz, CA) and the secondary antibody goat anti-mouse IgG – HRP (Santa Cruz; Santa Cruz, CA). β-actin is the loading control (Sigma-Aldrich; St. Louis, MO). The proteins were visualized using ECL western blot chemiluminescence kit (GE health care; Piscataway, NJ).

Modeling Studies

Computer-assisted simulated docking experiments were carried out under an MMFF94X force field in caspase-3 structure (PDB ID: 1GFW) using Chemical Computing Group's Molecular Operating Environment (MOE-dock 2009) software, Montréal, Canada.

RESULTS AND DISCUSSION

Chemistry

The synthetic strategies to obtain the target compounds are depicted in Schemes **1, 2** and **3**. Ethyl 4-cyano-1-oxo-1*H*,5*H*-pyrido[2,1-b]benzimidazol-3-acetate **(3**) and ethyl 4-cyano-1-oxo-1*H*-pyrido[2,1-b]benzothiazole-3-acetate **(4)** were prepared by fusion of 2-(1*H*-benzimidazol-2-yl)acetonitrile (**1**) [33] and 2-(benzothiazol-2-yl)acetonitrile (**2)** [34] with diethyl acetone-1,3-dicarboxylate in the presence of ammonium acetate at 140-150 °C, respectively. 2-(Benzothiazol -2-yl)acetonitrile **(2)** was fused with ethyl cyclohexanone-2-carboxylate in the presence of ammonium acetate to afford 7,8,9,10-tetrahydro-11-oxo-11*H*-benzothiazolo[3,2-b]isoquinoline-6-carbonitrile (**5**). Reacting **2** with 4-chlorobenzaldehyde and 4-chloroacetophenone in dry dioxane in the presence of ammonium acetate following reported reaction method [35] yielded the corresponding 2-[4,6-bis(4-chlorophenyl)-2-imino-1*H*-pyridin-3-yl]benzothiazole **(6)** (Scheme **1**).

Scheme **2** starts with the key intermediate, 2-(1*H*-benzimidazol-2-yl)acetimidohydrazide **(7)** which was prepared by refluxing **1** in excess hydrazine hydrate. Cyclization of the amidrazone derivative **7** was performed by refluxing with thionyl chloride, ethyl chloroformate or ethyl bromoacetate in ethanol and sodium ethoxide to obtain 1,2,3,5-thiatriazole derivative **8**, 1,2,4-triazol-3-one derivative **9** and 1,2,4-triazin-5-one derivative **10**, respectively.

The precursor *N*-(1*H*-benzimidazol-2-yl)-1*H*-imidazole-1-carboxamide **(12)** was prepared in analogy to a previously reported method [33,34] by reaction of 2-amino-1*H*-benzimidazole **(11)** with 1,1'-carbonyldiimidazole in acetonitrile. 1-(4-Methoxyphenethyl)-3-(1*H*-benzimidazol-2-yl)urea **(13)**, 1-(1*H*-benzimidazol-2-yl)-3-cyclohexylurea **(14)** and 1-(1*H*-benzimidazol-2-yl)-3-(4-methoxyphenyl)urea **(15)** were prepared by reacting **12** with the appropriate amines namely; 2-(4-methoxyphenyl)ethanamine, cyclohexylamine or 4-methoxy benzenamine in DMF, respectively (Scheme **3**).

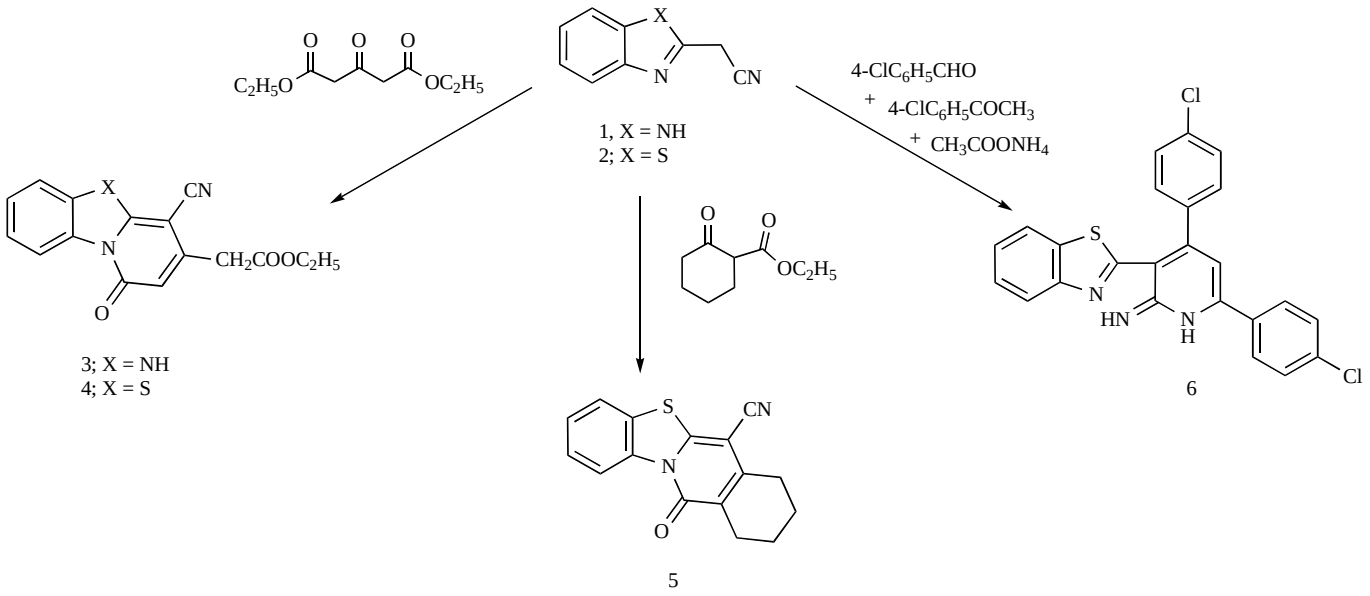

Scheme 1.

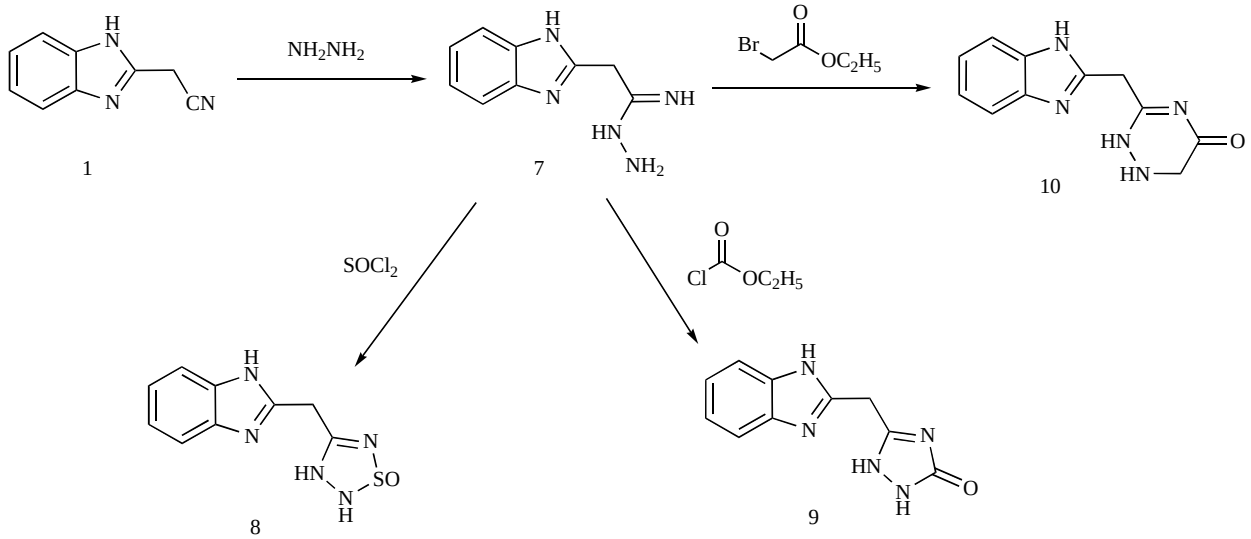

Scheme 2.

Anticancer Studies

Chemoprevention is now regarded as a promising strategy to control cancer [36]. Cancer is usually associated with aberrant cell cycle progression and defective apoptosis induction due to the activation of proto-oncogenes and/or inactivation of tumor suppressor genes [37]. We screened our novel derivatives against various cancer cell lines including breast cancer cells (MCF-7), colon cancer cells (RKO), lung cancer cells (H1299), Melanoma (B16F10) and liver cancer cells (HepG2), our initial screening study showed benzimidazole derivatives decreased proliferation of liver cancer cells (HepG2) (data not shown). In this study, we report novel benzimidazole and benzothiazole derivatives that showed cytotoxicity against liver cancer HepG2 cells.

Hepatocellular carcinoma (HCC) is one of the most common malignant tumor worldwide and in Egypt as well [38,39]. Despite the combined efforts of governments and scientists worldwide, there is constant increase in the incidence of Hepatocelluar carcinoma during the last two decades [40]. Successful drug treatment of a human disease requires an adequate therapeutic index reflecting the treatment's specific effects on target cells and its lack of clinically significant effects on the host. In the present study, a series of benzimidazole and benzothiazole derivatives were designed and synthesized to examine their effects on viability and proliferation in HepG2, liver cancer cell lines. The concentrations at which 50% inhibition of HepG2 cell viability (IC_{50}) were calculated using a semilogarithmic plotting of the % of cell viability *versus* concentration of the tested compounds. The (IC_{50} = 0.2~ 0.25 mM) dose of synthesized compounds **(3, 4, 5, 7, 8, 9,** and **10)** showed significant decrease in cell survival of HepG2 cells compared to control group (Fig. **1**).

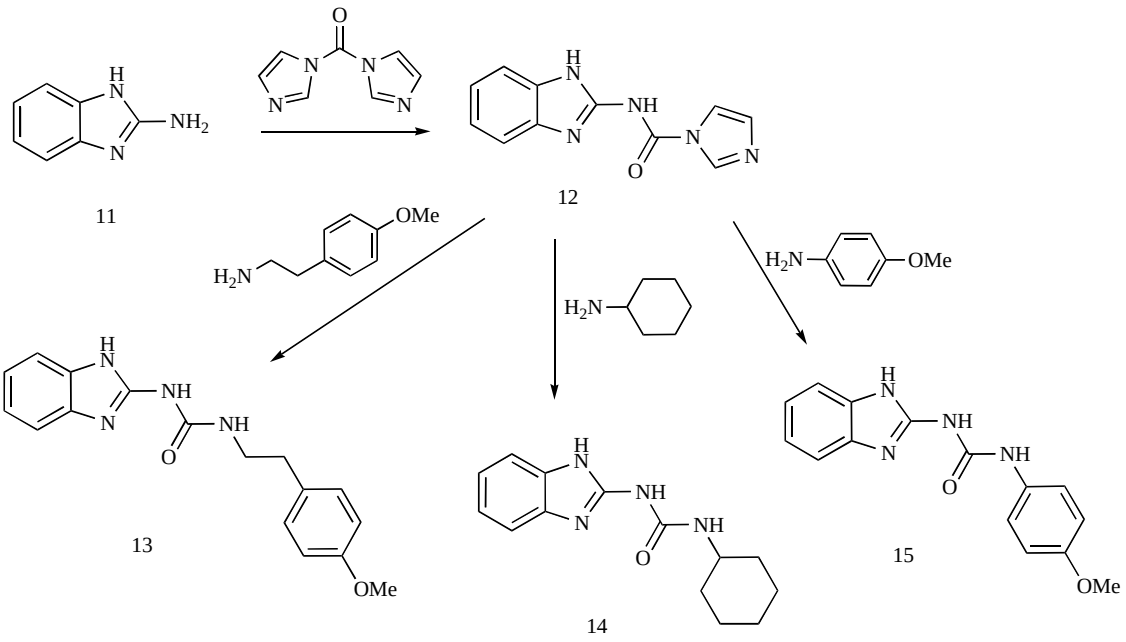

Scheme 3.

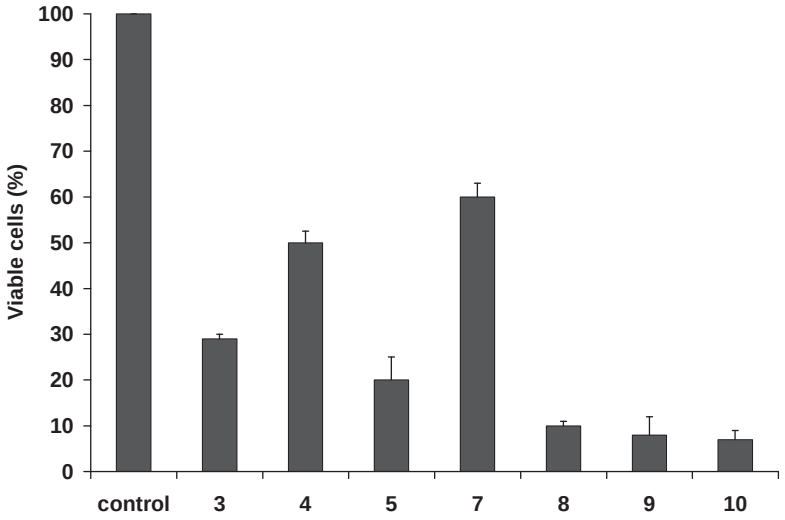

Fig. (1). Effect of benzimidazole and benzothiazole derivatives on cell viability of HepG2 cells. MTT assay was performed to detect living cells. Each data point is an average of results from three independent experiments performed in triplicate and presented as M±SD.

The cell viability of the most potent derivatives **(3, 5, 8, 9,** and **10)** was tested via the 3-(4,5-Dimethylthiazol-2-yl)-2,5-diphenyltetrazolium bromide assay (MTT) and the effects of compounds were confirmed. Our data showed a significant decrease in cell viability of HepG2 cells in dose dependent manner, using (IC_{50} range = 0.2~ 0.25 mM) dose that was determined based on dose response curve as shown in Fig. (**2**).

In addition to the previous tested compounds, we examined the effect of different series of compounds **(6, 12, 13, 14,** and **15)** on cell viability of HepG 2 cells. Our data indicated that compounds **12, 13,** and **14** significantly decreased cell viability compared to control group (Fig. **3**).

It is possible that the decrease in cell viability as determined by the tested compounds could be due to either cell growth arrest or cell death. Understanding the epdimiological factors and molecular mechanism associated with hepatocelluar carcinoma improves screening and treatment of the disease [41]. To investigate if the decrease in cells viability could be due to induced-apoptosis, Enzyme linked immunosorbent apoptosis assay (ELISA) was performed, which detected histone release from apoptotic cells. We next examined whether the tested compounds at toxic concentrations induced cell death or not. HepG 2 cells were treated with (IC_{50} = 0.2~ 0.25 mM) dose of compounds **(8, 9, 10, 12, 13,** and **14)** and induction of apoptosis was determined as indicated by histone release according to manufacturer's protocol. Our data indicated that previously mentioned derivatives significantly induced apoptosis in HepG2 cells compared to control untreated group (Fig. **4**).

Cell death was assayed by trypan blue staining, which determines membrane integrity. Compounds **(8, 9, 10, 12,**

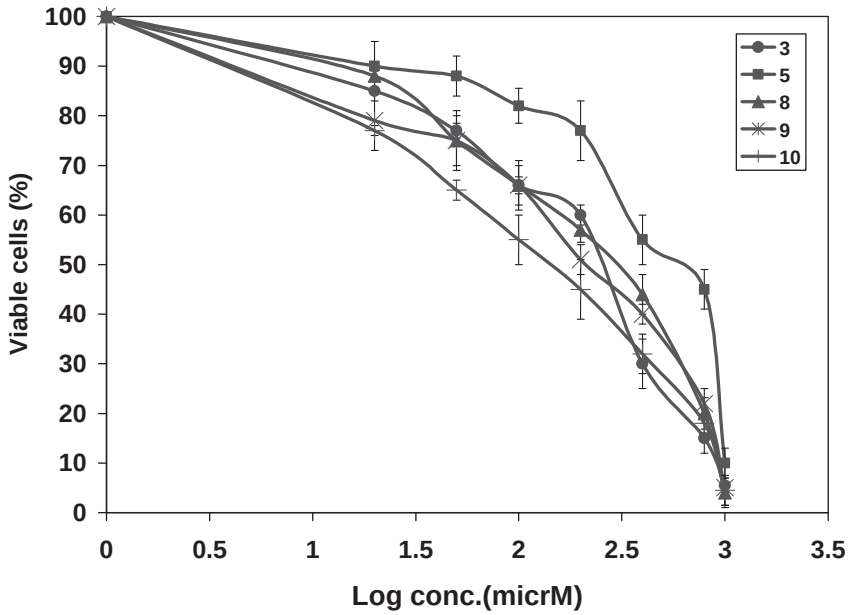

Fig. (2). Dose response curve of the tested compounds for HepG2 cells. Each data point is an average of three independent experiments and expressed as M±SD.

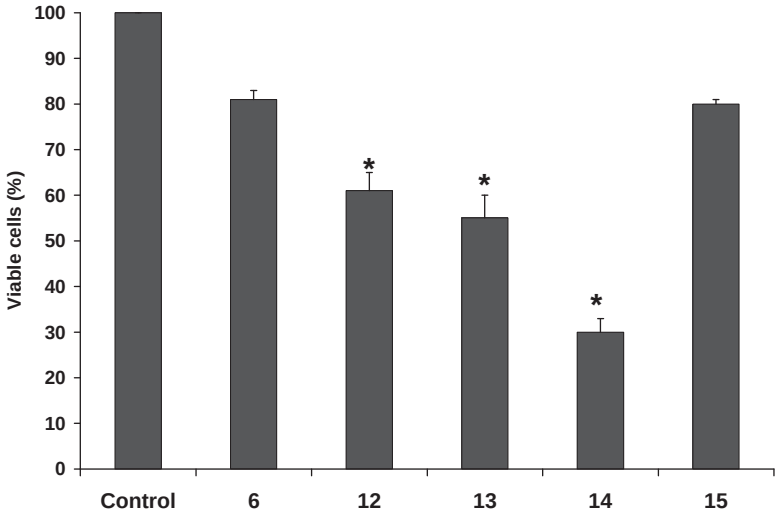

Fig. (3). Effect of benzimidazole and benzothiazole derivatives on cell viability of HepG2 cells. Each data point is an average of three independent experiments and expressed as M±SD.

13, and **14)** induced cell death was a relatively late event, occurring only after 24 h of treatment with 200 μM. The number of both the trypan blue-positive cells and the condensed and fragmented nuclei increased with compounds **(8, 9, 10, 12, 13,** and **14)** treatment (data not shown), confirming that the tested compounds-induced cell death was due to apoptosis in HepG 2 cells.

Because of the diversity of its substrates, caspase-3 is thought to be a general mediator of physiological as well as stress-induced apoptosis [42,43]. To investigate if the tested compounds would activate caspase-3 in treated HepG2 cells, Caspase-3 activity was assayed according to manufacturer's protocol (more details under the materials and methods). Our data indicated that the compounds **(8, 9, 10, 12, 13,** and **14)** showed a significant increase in caspase-3 activity in treated HepG2 cells when compared with untreated group.

As shown in Fig. (**5**) the tested compounds **(8, 9, 10, 12, 13,** and **14)** at the apoptosis-inducing concentration (IC_{50} range = 0.2~ 0.25 mM) dose strongly stimulated caspase-3-like activity in HepG2 cells. These results demonstrate that the active tested compounds induce apoptosis of HepG2 cells in a caspase-dependent manner.

Cell cycle checkpoints in G1 and G2 are activated in response to UV or gamma radiation allowing time for DNA repair to take place. After complete repair, the cells resume cycling. When the damage in cells is severe and cannot be repaired, the cells undergo apoptosis and die. Mammalian cell cycle is regulated by complex machinery, in which cyclin depenedent kinases (CDKs), cyclin depenedent kinase inhibitors (CDKIs) and cyclins play essential roles [44]. The increased expression of G1 cyclins in cancer cells provide them an uncontrolled growth advantage because most of

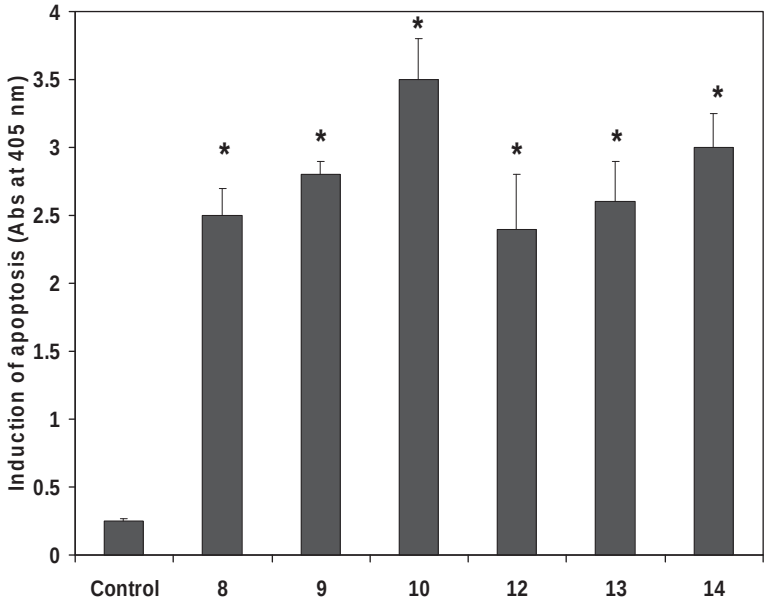

Fig. (4). ELISA assay was applied for apoptotic cell detection. Cells were treated with (IC_{50} range = 0.2~ 0.25 mM) dose of **8, 9, 10, 12, 13** d **14** for 24 h. Cells without drug treatment were used as controls. * $p < 0.05$ as compared to the mock-treated controls using the unpaired Student t-test. Each condition was performed in triplicate. Data are presented as M±SD.

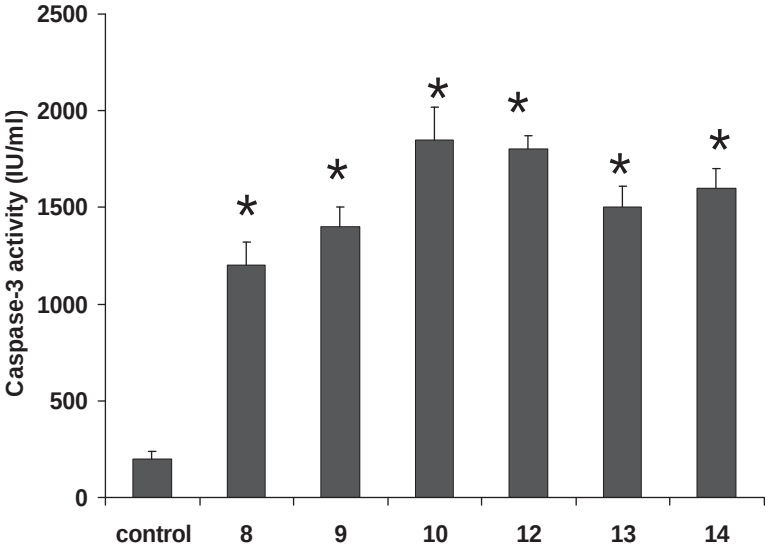

Fig. (5). Effect of benzimidazole derivatives on caspase-3 activity (As indicated by (DEVD-pNA) cleavage) in HepG2 cells in the presence of 200 μM. Each data point is an average of three independent experiments and expressed as M±SD.

these cells either lack CDKI or possess non-functional CDKI or have low expression of CDKI [45]. Consistent with the results from ELISA, sub-G1 apoptotic cells were shown by flow cytometry assay to have a significant increase in HepG2 cells (~ 30 and 25 % compared to the non-treated control of ~ 19%) by arresting cells in G1 phase (45 and 40% compared by untreated group) (Fig. **6A**). p21, a key regulator of G1 phase, was determined by Western blot analysis, our data indicated that both derivatives **10** and **12** increased its expression by 2 and 2.7 fold; respectively compared to control group (Fig. **6B, C**). Our data indicated that two benzimidazole derivatives **10** and **12** induced apoptosis compared to control group via arresting cells in G1 phase of cell cycle, increasing p21 expression level and increasing caspase-3 activity.

Docking Study

The docking study was carried out for the two active benzimidazole derivatives **10** and **12** using the enzyme parameters obtained from the crystallographic structure of the complex between caspase-3 with the co-crystallized isatin sulfonamide derivative MSI (PDB ID: 1GFW) [46]. The docking simulation for the ligands was carried out using molecular operating environment (MOE) software supplied by the Chemical Computing Group, Inc., Montréal Canada [47].

The x-ray co-crystal structure of the complex between recombinant human caspase-3 and isatin sulfonamide reveals that a tetrahedral intermediate is formed between the catalytic cysteine thiolate and the isatin ketone carbonyl group. The three hydrophobic residues (Tyr204, Trp206, and

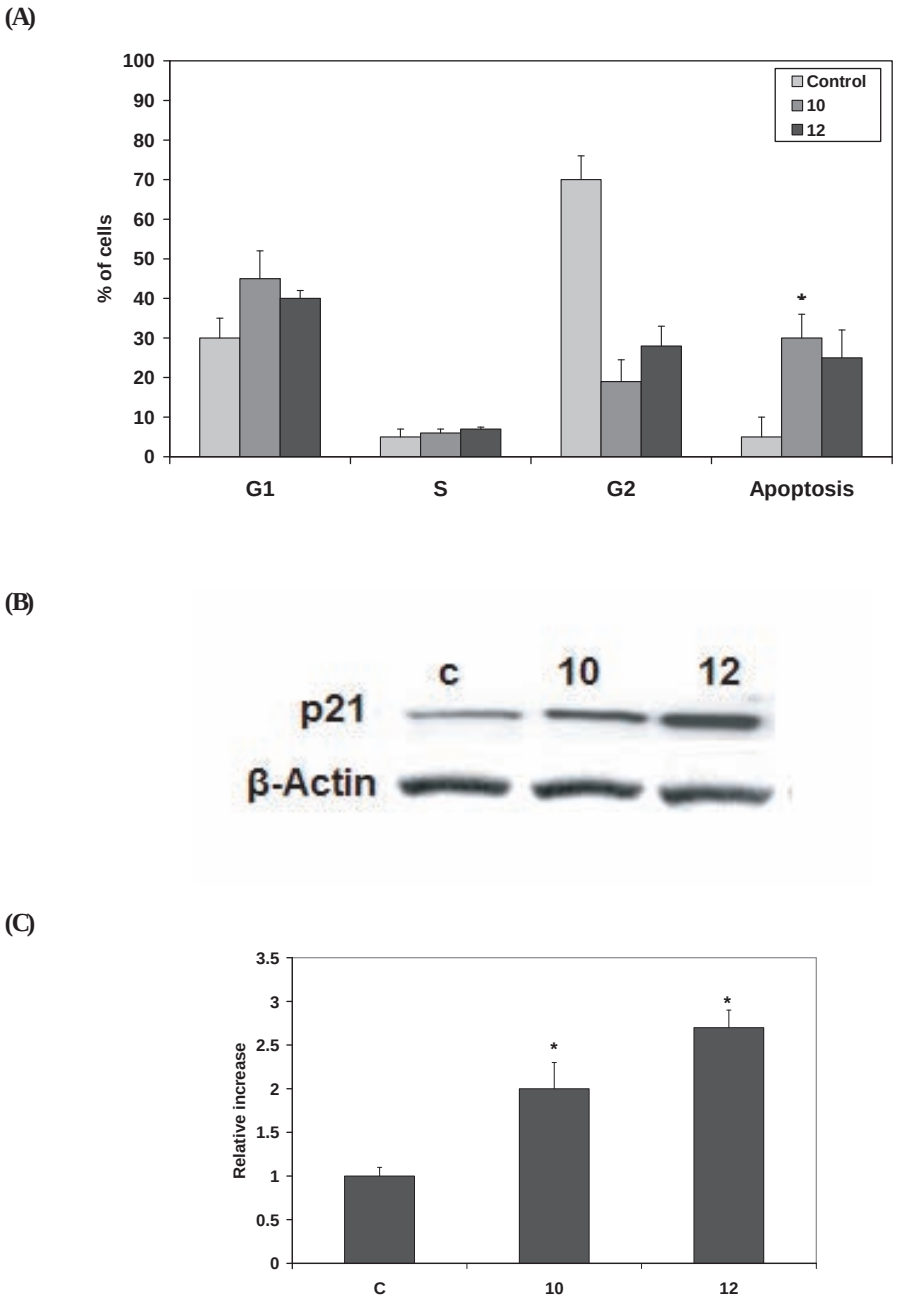

Fig. (6). Effect of benzimidazole derivatives on cell cycle progression. Cells were treated as described under the materials and methods. The % of cell cycle phases was determined in HepG2 cells after treatment with 200 μM of **10** and **12** for 24 h (**A**). Expression level of p21 was determined for p21 after treating cells with the same concentration of derivatives 10 and 12 and β-actin was used as control (**B**). Relative increase in p21 expression was illustrated as bar graph and data are presented as M±SD (**C**).

Phe256) in the S_2 pocket are involved in extensive hydrophobic contacts with the pyrrolidine ring of the inhibitor. In the caspase-3/inhibitor MSI structure, the oxygen of the tetrahedral intermediate and the amide carbonyl oxygen are within hydrogen bonding distance of Cys163NH and Gly122NH, respectively. There is a hydrophobic and/or aromatic interaction between the edge of Tyr204 with one face of the bicyclic isatin core, which likely contributes to the binding of the inhibitor. Whereas in compound **10**, hydrogen bonding is observed between nitrogen of triazine ring and Cys163NH as well as Gly122NH. Hydrogen bonding is also seen between nitrogen of triazine ring and carbonyl oxygen of Gly122. The bezimidazole ring of compound **10** is bound in a hydrophobic cavity formed by Tyr204 and Phe256 (Fig. **7**).

Fig. (**8**). shows caspase-3 superimposition of MSI and the docked compound **12**. In this case, hydrogen bonding is observed between the amide carbonyl oxygen of compound **12** and both the NH of Cys163 and Gly122. Hydrogen bonding is also seen between the nitrogen of imidazole ring of compound **12** and Arg207NH as well as Arg64NH. The benzimidazole ring is surrounded by hydrophobic residues Gly165, Thr166 and Ser205.

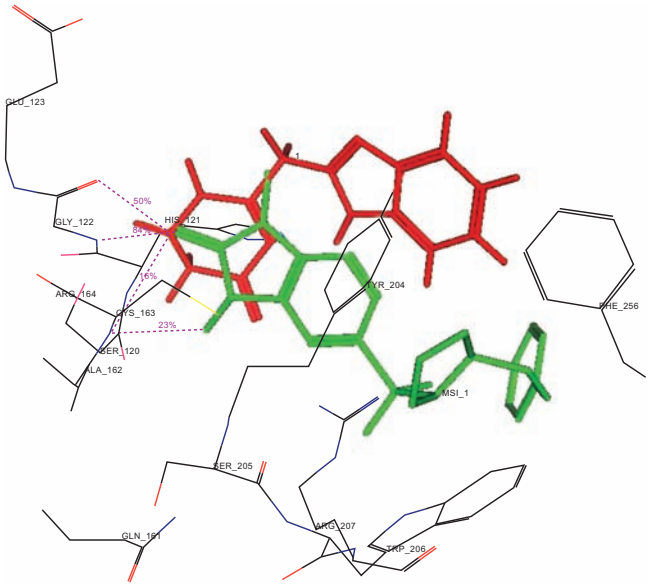

Fig. (7). Caspase-3 superimposition of the co-crystallized isatin derivative MSI (colored green) and the docked compound **10** (colored red). Pink dashed lines depict hydrogen bond interactions. Viewed using MOE module. (For interpretation of the references to color in this figure legend, the reader is referred to the web version of this paper).

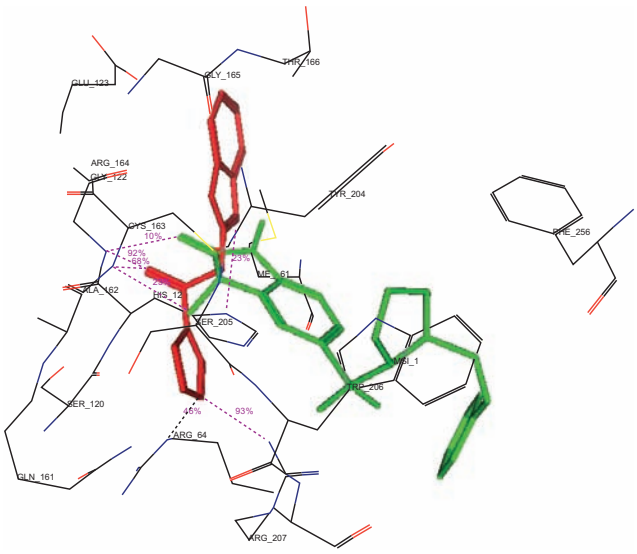

Fig. (8). Caspase-3 superimposition of the co-crystallized isatin derivative MSI (colored green) and the docked compound **12** (colored red). Pink dashed lines depict hydrogen bond interactions. Viewed using MOE module. (For interpretation of the references to color in this figure legend, the reader is referred to the web version of this paper).

The docking study shows that compounds **10** and **12** form hydrogen bonds with the same residues (Cys163 and Gly122) as that observed in the crystal structure of the MSI complex. Moreover, compound **10** have a binding pattern in the caspase-3 site which is close to the pattern observed in the crystallographic structure of the complex between caspase-3 with the co-crystallized isatin sulfonamide derivative MSI. This may account for increased caspase-3 activity recorded for compound **10**.

Structure-Activity Relationship

We can contrive from the anticancer studies together with docking studies that the benzimidazole nucleus is responsible for the traced activity as it is responsible for the interaction with hydrophobic residues of the enzyme, on condition that the spacer between this ring and the SP^2 nitrogen atom or its isoster does not exceed two carbon atoms. Elongation of the spacer might decrease or abolish the activity.

CONCLUSION

In conclusion, our novel benzimidazole series of compounds exhibit cytotoxicity to HepG2 and induced apoptosis via activation of caspase-3 activity which is confirmed by docking experiments. Additionally, they increased expression of p21 as key play in cell cycle by arresting cells in G1

arrest inducing cells to apoptosis. Mutations or loss of caspase-3 leads to a blockade of of apoptosis and DNA fragmentation in different cancer cell lines. Therefore, the caspase-dependent apoptotic effect of the tested compounds may be of clinical relevance in determining sensitivity versus resistance of liver cancer cells to such tested compounds since activation of caspase-3 is known to increase sensitivity of cancer cells to treatment. Based on our docking experiments, these analogs will enable us to examine important structural determinants of small molecule macromolecular interactions for anticancer activity. The discovery of a class of highly selective and potent benzimidazole derivatives will lead to development of new anticancer drugs. Moreover, *in vivo* studies are required to determine whether benzimidazole series could be an effective chemotherapeutic agent for treatment of Hepatocelluar carcinoma (HCC).

REFERENCES

[1] Unger, C. New therapeutics approaches in cancer treatment. *Drug Future*, **1997**, *22*, 1337-45.

[2] Melén, K.; Keskinen, P.; Lehtonen, A.; Julkunen, I. Interferon-induced gene expression and signaling in human hepatoma cell lines. *J. Hepatol.*, **2000**, *33*, 764-72.

[3] Simstein, R.; Burow, M.; Parker, A.; Weldon, C.; Beckman, B. Apoptosis, chemoresistance, and breast cancer: insights from the MCF-7 cell model system. *Exp. Biol. Med.*, **2003**, *228*, 995-1003.

[4] Galal, S.A.; Hegab, K.H.; Hashem, A.M.; Youssef, N.S. Synthesis and antitumor activity of novel benzimidazole-5-carboxylic acid derivatives and their transition metal complexes as topoisomerease II inhibitors. *Eur. J. Med. Chem.*, **2010**, *45*, 5685-91.

[5] Desai, G.K.; Desai, R.K. A facile microwave enhanced synthesis of sulfur-containing 5-membered heterocycles derived from 2-mercaptobenzothiazole over $ZnCl_2$/DMF and antimicrobial activity evaluation. *J. Sulfur Chem.*, **2006**, *27*, 315-28.

[6] Desai, G.K.; Desai, R.K. Green route for the heterocyclization of 2-mercaptobenzimidazole into beta-lactum segment derivatives containing -CONH- bridge with benzimidazole: screening in vitro antimicrobial activity with various microorganisms. *Bioorg. Med. Chem.*, **2006**, *14*, 8271-79.

[7] Gowda, N.R.; Kavitha, T.C.V.; Chiruvella, K.K.; Joy, O.; Rangappa, K.S.; Raghavan, S.C. Synthesis and biological evaluation of novel 1-(4-methoxyphenethyl)-1H-benzimidazole-5-carboxylic acid derivatives and their precursors as antileukemic agents. *Bioorg. Med. Chem. Lett.*, **2009**, *19*, 4594-600.

[8] Schulz, W.G.; Islam, I.; Skibo, E.B. Pyrrolo[1,2-a]benzimidazole-based quinones and iminoquinones. The role of the 3-substituent on cytotoxicity. *J. Med. Chem.*, **1995**, *38*, 109-18.

[9] Islam, I.; Skibo, E.B. Synthesis and physical studies of azamitosene and iminoazamitosene reductive alkylating agents. Iminoquinone hydrolytic stability, syn/anti isomerization, and electrochemistry. *J. Org. Chem.*, **1990**, *55*, 3195-205.

[10] Islam, I.; Skibo, E.B.; Dorr, R.T.; Alberts, D.S. Structure-activity studies of antitumor agents based on pyrrolo[1,2-a]benzimidazoles: new reductive alkylating DNA cleaving agents . *J. Med. Chem.*, **1991**, *34*, 2954-61.

[11] Skibo, E.B.; Schulz, W.G. Pyrrolo[1,2-a]benzimidazole-based aziridinyl quinones. A new class of DNA cleaving agent exhibiting G and A base specificity. *J. Med. Chem.*, **1993**, *36*, 3050-55.

[12] Skibo, E.B.; Islam, I.; Alberts, D.S. Antineoplastic compounds and methods of using same. U.S. Patent 5,246,955, **1993**; Chem. Abstr. **1994**, *119*, 214369q.

[13] Skibo, E.B.; Islam, I.; Heileman, M.J.; Schulz, W.G. Structure-activity studies of benzimidazole-based DNA-cleaving agents. Comparison of benzimidazole, pyrrolobenzimidazole, and tetrahydropyridobenzimidazole analogues. *J. Med. Chem.*, **1994**, *37*, 78-92.

[14] Skibo, E.B. Synthesis and elucidation of azamitosene and iminoazamitosene. U.S. Patent 5,015,742, **1991**; Chem. Abstr. **1991**, *115*, 183297n.

[15] Boruah, R.C.; Skibo, E.B.A Comparison of the cytotoxic and physical properties of aziridinyl quinone derivatives based on the pyrrolo[1,2-a] benzimidazole and pyrrolo[1,2-a] indole ring systems. *J. Med. Chem*., **1994**, *37*, 1625-31.

[16] Chen, A.Y.; Yu, C.; Gatto, B.; Liu, L.F. DNA minor groove-binding ligands: a different class of mammalian DNA topoisomerase I inhibitors. *Proc. Natl. Acad. Sci. U.S.A.*, **1993**, *90*, 8131-35.

[17] Chen, A.Y.; Yu, C.; Bodley, A.; Peng, L.F.; Liu, L.F. A new mammalian DNA topoisomerase I poison. Hoechst 33342: cytotoxicity and drug resistance in human cell cultures .*Cancer Res.*, **1993**, *53*, 1332-37.

[18] Pourgholami, M.H.; Woon, L.; Almajd, R.; Akhter, J.; Bowery, P.; Morris, D.L. *In vitro* and *in vivo* suppression of growth of hepatocellular carcinoma cells by albendazole. *Cancer Lett.*, **2001**, *165*, 43-9.

[19] Mortimer, C.G.; Wells, G.; Crochard, J.P.; Stone, E.L.; Bradshaw, T.D.; Stevens, M.F.G.; Westwell, A.D. Antitumor benzothiazoles. 26. 2-(3,4-Dimethoxyphenyl)-5-fluorobenzothiazole (GW610, NSC 721648), a simple fluorinated 2-arylbenzothiazole, shows potent and selective inhibitory activity against lung, colon, and breast cancer cell lines. *J. Med. Chem*.**, 2006**, *49*, 179-85.

[20] Yoshida, M.; Hayakawa, I.; Hayashi, N.; Agatsuma, T.; Oda, Y.; Tanzawa, F.; Iwasaki, S.; Koyama, K.; Furukawa, H.; Kurakata, S.; Sugano, Y. Synthesis and biological evaluation of benzothiazole derivatives as potent antitumor agents. *Bioorg. Med. Chem. Lett.*, **2005**, *15*, 3328-32.

[21] Ćaleta, I.; Kralj, M.; Marjanović, M.; Bertosa, B.; Tomić, S.; Pavlović, G.; Pavelić, K.; Karminski-Zamola, G. Novel cyano- and amidinobenzothiazole derivatives: synthesis, antitumor evaluation, and X-ray and quantitative structure-activity relationship (QSAR) analysis. *J. Med. Chem.*, **2009**, *52*, 1744-56.

[22] Chung, Y.; Shin, Y.K.; Zhan, C.G.; Lee, S.; Cho, H. Synthesis and evaluation of antitumor activity of 2- and 6-[(1,3-benzothiazol-2-yl)aminomethyl]-5,8-dimethoxy-1,4-naphthoquinone derivatives. *Arch. Pharm. Res.*, **2004**, *27*, 893-900.

[23] Kok, S.H.L.; Gambari, R.; Chui, C.H.; Yuen, M.C.W.; Lin, E.; Wong, R.S.M.; Lau, F.Y.G.; Cheng, Y.M.; Lam, W.S.; Chan, S.H.; Lam, K.H.; Cheng, C.H.; Lai, P.B.S.; Yu, M.W.Y.; Cheung, F.; Tang, J.C.O.; Chan, A.S.C. Synthesis and anti-cancer activity of benzothiazole containing phthalimide on human carcinoma cell lines. *Bioorg. Med. Chem.*, **2008**, *16*, 3626-31.

[24] Chua, M.-S.; Shi, D.-F.; Wrigley, S.; Bradshaw, T.D.; Hutchinson, I.; Shaw, P.N.; Barrett, D.A.; Stanley, L.A.; Stevens, M.F.G. Synthesis of 2-(4-acylaminophenyl)benzothiazoles and investigations into the role of acetylation in the antitumor activities of the parent amines. *J. Med. Chem.*, **1999**, *42*, 381-92.

[25] Kashiyama, E.; Hutchinson, I.; Chau, M.-S.; Stinson, S.F.; Phillips, L.R.; Kaur, G.; Sausville, E.A.; Bradshaw, T.D.; Westwell, A.D.; Stevens, M.F.G. Synthesis, metabolic formation, and biological properties of the C- and N-oxidation products of antitumor 2-(4-aminophenyl)benzothiazoles. *J. Med. Chem.*, **1999**, *42*, 4172-84.

[26] Shi, D.-F.; Bradshaw, T.D.; Wrigley, S.; McCall, C.J.; Lelieveld, P.; Fichtner, I.; Stevens, M.F.G. Synthesis of 2-(4-aminophenyl)benzothiazoles and evaluation of their activities against breast cancer cell lines *in vitro* and *in vivo*. *J. Med. Chem.*, **1996**, *39*, 3375-84.

[27] Ashkenazi, A.; Dixit, V.M. Death receptors signaling and modulation. *Science*, **1998**, *281*, 1305-8.

[28] O'Connor, L.; Harris, A.W.; Strasser, A. CD95 (Fas/APO-1) and p53 signal apoptosis independently in diverse cell types. *Cancer Res.*, **2000**, *60*, 1217-22.

[29] Burns, T.F.; Bernhard, E.J.; El-Deiry, W.S. Tissue specific expression of p53 target genes suggests a key role for KILLER/DR5 in p53-dependent apoptosis *in vivo*. *Oncogene*, **2001**, *601*, 4612-18.

[30] Jacobson, M. D.; Weil, M.; Raff, M.C. Programmed cell death in animal development. *Cell*, **1997**, *88*, 347-54.

[31] Liu, X.; Zou, H.; Slaughter, C.; Wang, X. DFF, a heterodimeric protein that functions downstream of caspase-3 to trigger DNA fragmentation during apoptosis. *Cell*, **1997**, *89*, 175-84.

[32] Datta, R.; Kojima, H.; Yoshida, K.; Kufe, D. Caspase-3-mediated cleavage of protein kinase C theta in induction of apoptosis. *J. Biol. Chem.*, **1997**, *272*, 20317-20.

[33] Grana, X.; Reddy, P. Cell cycle control in mammalian cells: role of cyclins, cyclin dependent kinases (CDKs), growth suppressor genes and cyclin-dependent kinase inhibitors (CKIs). *Oncogene*, **1995**, *11*, 211-9.

[34] Copeland, R.A.B.; Day, A.R. The preparation and reactions of 2-benzimidazolecarboxylic acid and 2-benzimidazoleacetic acid. *J. Am. Chem. Soc.*, **1943**, *65*, 1072-5.

[35] Saito, K.; Kambe, S.; Nakano,Y. Synthetic studies using α,β-unsaturated nitriles: a convenient preparation of 1,3-benzothiazole derivatives. *Synthesis*, **1983**, 210-2.

[36] Hengartner, M.O. The biochemistry of apoptosis. *Nature*, **2000**, *407*, 770-776.

[37] Hanahan, D; Weinberg, R.A. The hallmarks of cancer. *Cell*, **2000**, *100*, 57-70.

[38] El-Zayadi, A.R.; Abaza, H.; Shawky, S.; Mohamed, M.K.; Selim, O.E.; Badran, H.M. Prevalence and epidemiological features of hepatocellular carcinoma in Egypt-a single center experience. *Hepatol. Res*., **2001**, *19*, 170-9.

[39] Ohata, K.; Hamasaki, K.; Toriyama, K.; Ishikawa, H.; Nakao, K.; Eguchi, K. High viral load is a risk factor for hepatocellular carcinoma in patients with chronic hepatitis B virus infection. J. *Gastroenterol. Hepatol.*, **2004**, *19*, 670-5.

[40] Jemal, A.; Bray, F.; Center M.M.; Ferlay, J.; Ward, E.; Forman, D. Global cancer statistics. CA. *Cancer J. Clin.*, **2011**, *61*, 69-90.

[41] El-Serag, E.B.; Rudolph, K.L. Hepatocellular carcinoma: epidemiology and molecular carcinogenesis. *Gastroenterology*, **2007**, *132*, 2557-76.

[42] Kulik, L. M. Advancements in hepatocellular carcinoma. *Curr. Opin. Gastroenterology* , **2007**, *23*, 268-74.

[43] El-Serag, H.B. Hepatocellular carcinoma: recent trends in the united states. *Gastroenterology*, **2004**, *127*(Suppl 1) S27-S34.

[44] Ashkenazi, A.; Dixit, V.M. Death receptors: signaling and modulation. *Science*, **1998**, *281*, 1305-8.

[45] Dullic, V.; Lees, E.; Reed, S.I. Association of human cyclin E with a periodic G1-S phase protein kinase. *Science*, **1992**, *257*, 1958-61.

[46] Lee, D.; Long, S.A.; Adams, J.L.; Chan, G.; Vaidya, K.S.; Francis, T.A.; Kikly, K.; Winkler, J.D.; Sung, C-M.; Debouck, C.; Richardson, S.; Levy, M.A.; DeWolf, W.E.; Keller, Jr.P.M.; Tomaszek, T.; Head, M.S.; Ryan, M.D.; Haltiwanger, R.C.; Liang, P-H.; Janson, C.A.; McDevitt, P.J.; Johanson, K.; Concha, N.O.; Chan, W.; Abdel-Meguid, S.S.; Badger, A.M.; Lark, M.W.; Nadeau, D.P.; Suva, L.J.; Gowen, M.; Nuttall, M.E. Potent and selective nonpeptide inhibitors of caspases 3 and 7 inhibit apoptosis and maintain cell functionality. *J. Biol. Chem*., **2000**, *275*, 16007-14.

[47] Molecular Operating Environment (MOE) **2009.10**, Chemical Computing Group Inc., 1010 Sherbrooke Street West, Suite 910, Montréal, H3A 2R7, Canada, http://www.chemcomp.com

Received: June 02, 2011 Revised: November 05, 2011 Accepted: November14, 2011